BULLETIN OF THE EARTHQUAKE
RESEARCH INSTITUTE
Vol. 39, (1961), pp. 603-630

23. *Division of the South-western Pacific Area into Several Regions in each of which Rayleigh Waves Have the Same Dispersion Characters.*

By Tetsuo A. SANTÔ,

Earthquake Research Institute.

(Read July 28, 1961.—Received September 30, 1961.)

Abstract

In the previous papers, the writer classified the dispersion curves of Rayleigh waves into seven kinds, and gave them the characteristic numbers from "1" to "7". These curves were revealed to be not independent of each other. For example, when Rayleigh waves pass across three differing regions with dispersion characteristic numbers "1", "3" and "7" with a pass length ratio of 3:3:4, the resultant dispersion character along the total path shows the character "5". Similar relations could be found also with the other curves (Fig. 3).

Using these relations, a trial was made to divide the complicated oceanic area in the western side of the "Andesite line" into four regions "1" (purely oceanic type), "3" (sub-oceanic type), "5" (sub-continental type) and "7" (purely continental type).

At first, the present oceanic area was divided into four regions by using the dispersion data obtained along thirty-two paths for Tsukuba Station (Fig. 4). Secondly, the same work was done by adding other dispersion data along thirteen paths for three stations, Hongkong, Honolulu and Suva (Fig. 11).

In order to check the results, the group velocities of Rayleigh waves across these divided regions were calculated by least square method (Figs. 6, 12). The result showed that our division map was quite satisfactory.

Judging from the division map obtained, it was recognized that the crustal structure in the western side of the "Andesite line" was certainly more continental than in the eastern side of it. In the sea region deeper than 4 km, for instance, Rayleigh waves show the characteristic number "1" in the eastern side, while they show the sub-oceanic one "3" in the western side. The region in which Rayleigh waves show the dispersion characterized by type "1" is, in the western side of the "Andesite line", limitted to regions with a much greater ocean depth, the depth being greater than 6 km.

Rayleigh waves through the East China Sea or the Borneo Sea show the purely continental dispersion character "7". Only in the central part of the South China Sea or in small parts of the Celebes Sea, does the dispersion of Rayleigh waves show the sub-oceanic character "3".

Four kinds of dispersion curves in the divided regions were compared with the theoretical ones, and it was found that the shift of the dispersion character from "1" to "7" could be explained by decreasing the compressional waves velocity in the crust from 6.9 km/sec to 5.0 km/sec and by increasing the thickness of the crust from 5 km to 20 km. (Fig. 13).

1. Introduction

Four kinds of seismological methods have often been used to determine the crustal structure of the earth. The first two are the "reflected or refracted wave method" that is, the method by observing the reflected or refracted body waves which are generated at some discontinuity near the surface of the earth. The other two are based upon the observation of surface wave dispersions, which is classified into two. The first one is the "phase velocity method", that is, the method by observing the dispersive character of phase velocity and the other the "group velocity method" by observing that of group velocity.

Among these, the last method has very often been used by many seismologists on account of its simplicity. This method, however, has its own weakness, *i.e.*, what it gives us is an information only about the average crustal structure along a path between an epicenter and an observation station. For this reason, when the path covers various regions with different crustal structures, this method gives us no information about these local crustal structures.

The present writer has made investigations into the dispersion of Rayleigh waves along the various oceanic paths to Japan by using the records of the Columbia-type seismograph at Tsukuba Station[1),2),3)]. The most interesting fact which attracted our attention was that the

1) T. A. SANTÔ, "Observation of Surface Waves by Columbia-type Seismograph Installed at Tsukuba Station, Japan (Part I).—Rayleigh Wave Dispersions across the Oceanic Basin—." *Bull. Earthq. Res. Inst.*, **38** (1960), 219.

2) T. A. SANTÔ, "Rayleigh Wave Dispersions across the Oceanic Basin around Japan (Part II)." *Bull. Earthq. Res. Inst.*, **38** (1960), 385.

3) T. A. SANTÔ, "Rayleigh Wave Dispersions across the Ocean Basin around Japan (Part III)—On the Crust of the South-western Pacific Ocean—." *Bull. Earthq. Res. Inst.*, **39** (1961), 1.

dispersive character of Rayleigh waves changed remarkably in the south western Pacific Ocean. The result is shown in Figs. 1 and 2, in which the number beside each curve and travelling path means the characteristic number which the writer gave to each individual dispersion curve, from the typical oceanic one ("1") to the typical continental one ("7") in this order.

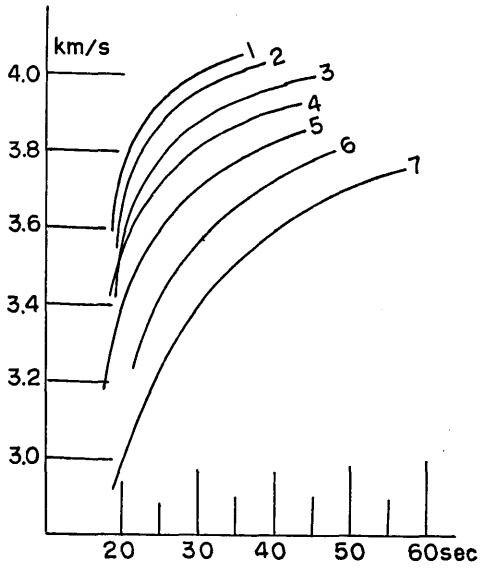

Fig. 1. Seven kinds of dispersion curves.

As is known, there runs a line, called the "Andesite line", in the south-western Pacific region (see the chain line in Fig. 2) which separates the region of predominantly andesitic volcanism from the region of the oceanic basin of predominantly basaltic volcanism. However, it has not been surveyed to ascertain whether or not the continental crustal condition just at the western side of the line continues over the whole area in this side. For this reason, it becomes very interesting that the

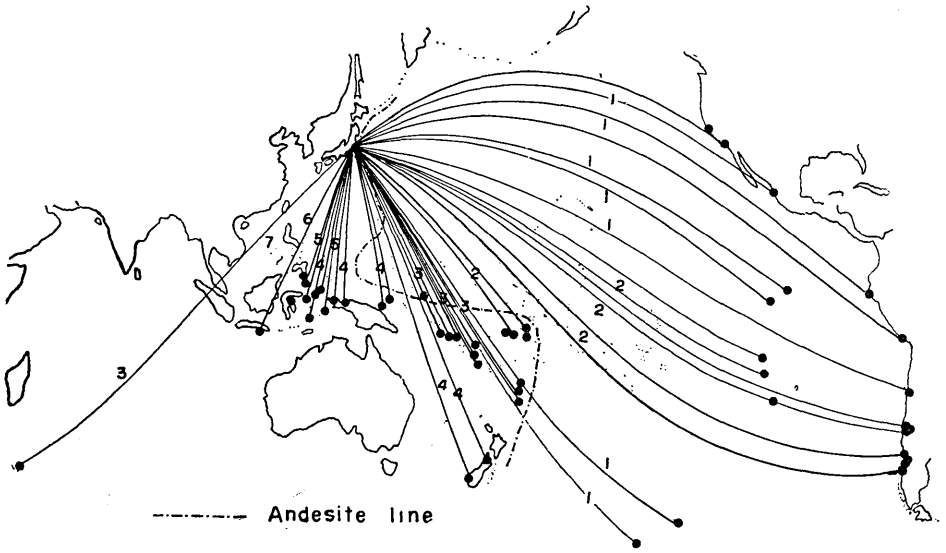

Fig. 2. Main travelling paths of Rayleigh waves across various oceanic paths.

dispersion character of Rayleigh waves on this side changes gradually from "2" to "7" with the shift of the travelling path westward.

From this observational fact concerning the dispersion character together with the complicated geographical conditions, we can suggest that the crustal structure in this area will be very complicated and has a lateral variation along the travelling paths to Tsukuba. In other words, the Rayleigh waves along a path across this area must have travelled through each region with different velocities. Therefore, the dispersion data observed at Tsukuba along these paths are nothing but an averaged ones, though the paths are all ocanic ones.

The present work is a trial to discover some regions in each of which the Rayleigh waves may have the same dispersive character.

2. Method of dividing the oceanic area into some regions in each of which Rayleigh waves have the same group velocity dispersion character.

When Rayleigh waves pass across two regions A and B, for instance, with different crustal structures, the resultant group velocity V can be found by the following simple relation, $k\Delta/V_A+(1-k)\Delta/V_B=\Delta/V$, in which, V_A and V_B are the group velocities of Rayleigh waves across A and B regions respectively and k is the ratio of the path length over the region A to the total one Δ. Therefore, if we know two kinds of dispersion curves for these two regions, we can obtain the resultant group velocity V for each period as well as the resultant dispersion curves for various values of k. The broken curves in Fig. 3 mean some examples which were obtained by this method for $k=0.2$, 0.4, 0.6 and 0.8 when the composing two regions are "1" (it means the region in which Rayleigh waves show the dispersion character of "1") and "5" (diagram a), "1" and "6" (diagram b), etc. Some observed dispersion curves are given in these diagrams, for comparison, using thick solid curves. From these results, the following relations can be recognized: The resultant dispersion curve "5" (see diagram b), for instance, can be considered to be a resultant one when Rayleigh waves have passed across the regions "1" and "6" with a ratio of path length approximately 3 : 7 respectively. Further, from the diagram d, the dispersion curve "6" can be considered to be a resultant one when Rayleigh waves have passed across the regions "4" and "7" with a path length ratio of 4 : 6. Therefore, if we combine these two relations given above, the dispersion character "5" can also be considered to be a resultant one when Rayleigh waves

have passed across three regions "1", "4" and "7" with a path length ratio of approximately 3 : 3 : 4. Similar relations can be found for any other curve.

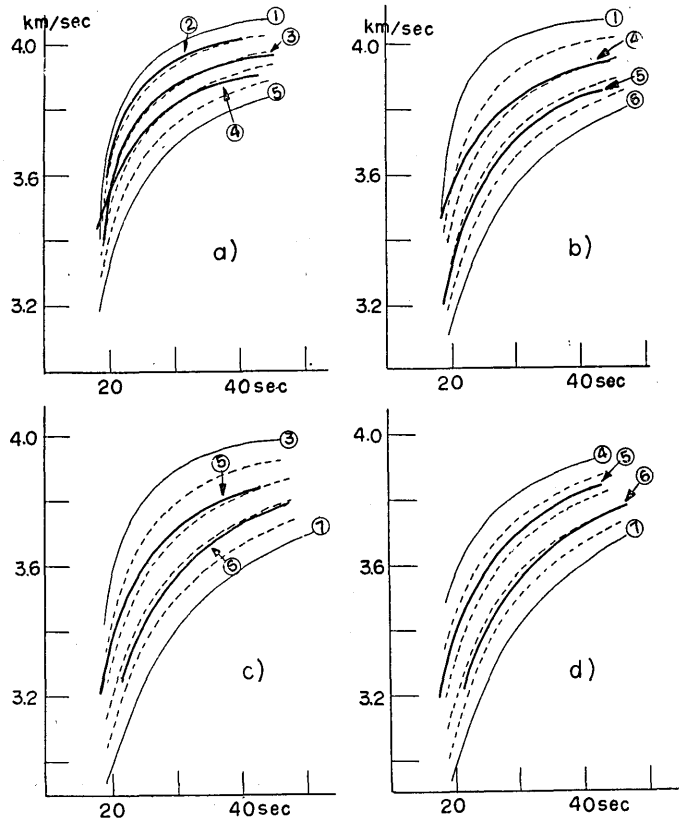

Fig. 3. Some examples which show the relation between seven kinds of dispersion curves.

These relations which hold between the seven kinds of dispersion curves are important ones, which give us a method for discovering the regions of differing dispersive character in the present area by using inversely the relations given above. Namely, if we assume some regions along a travelling path, we can divide each path into the parts belonging to these regions with such suitable path lengths as to make the resultant dispersion character along the total path into an observed one.

We must assume at first, a few kinds of regions from which the present area may be composed. The most oceanic and continental ones "1" and "7" must of course be selected. As has been reported in the

previous paper, the dispersion curve through the Indian Ocean shows "3", differing from that in the central Pacific Ocean ("1"). Therefore, the region, *i.e.*, the curve "3", was selected as a "sub-oceanic" one which represents the crustal condition *i.e.*, the dispersion character, in

Table 1.

No.	N	District	Epicenter	Origin Time (G.M.T.)	Date	Δ (km)	h (km)	M
29	6	Java I.	9.5S 112.5E	01h11m30s	Oct. 20,58	5850		
77	3	Mindanao I.	7 N 126.5E	18 01 30	Sept. 11,58	3550		
101	5	Celebes I.	1 N 123 E	09 34 00	Dec. 02,59	3500		6.5
56	5	Molluca passage.	2 S 126.5E	20 15 33	July 22,59	4060		
125	3	Helmahera Is.	1 N 129 E	02 22 06	Mar. 06,60	4080		
114	4	Ceram Is.	4 S 127.5E	04 40 56	Jan. 23,60	4700		6.5
115	4	〃	〃	17 56 30	〃	〃		
217	5	Timor Is. region	7.6S 128.8E	22 27 52.7	Aug. 16,60	5010	63	
34	5	Banda Sea	6 S 131 E	13 48 20	Nov. 14,58	4780		
21	4	New Guinea	3.5S 135.5E	07 19 16	May 01,59	4480		
126	4	〃	3 S 138 E	19 15 37	Mar. 19,60	4390		
221	4	Solomon Is.	10.3S 161.2E	08 22 00.7	Oct. 22,60	5570		6.5
138	4	Norfolk Is.	28 S 167.5E	11 12 31	May 20,60	7650		6.5
207	3	Solomon Is.	11.2S 163.1E	14 04 31.9	Sept. 10,60	5750	48	
116	3	Santa Cruz Is.	11.5S 166.5E	20 56 08	Feb. 11,60	5950		
216	3	〃	12.4S 166.4E	23 36 51.5	Aug. 09,60	5980	80	
238	3	〃	12.4S 166.3E	10 11 56.9	Jan. 02,61	6060	161	6.8
127	3	Loyality Is.	22.5S 174 E	15 19 30	Mar. 30,60	7400		
119	3	Fiji Is.	20 S 174.5E	16 14 47	Nov. 28,59	7180		
123	3	〃	19.5S 174.5E	02 45 45	〃 28,59	7140		
111	4	South I. of New Zealand	42 S 173 E	00 46 56	Feb. 21,60	9270		
12	3	〃	29.5S 176.5W	14 19 51	Oct. 29,59	8550		6.5
9	3	Kermadec Is.	29 S 177 W	22 23 53	Sept. 14,59	8500		6.5
10	3	〃	〃 176.5W	15 31 57	〃 29.59	8510		6.5
206	3	Tonga Is.	27.6S 176.9W	07 35 22	〃 01,60	8480	500	
13	3	〃	24 S 176.5W	13 15 49	〃 14,59	8100		
227	3	South of Tonga Is.	24.2S 176.1W	14 12 21.1	Nov. 23,60	8125	28	7
205	2	Fiji Is.	16.1S 179.6W	20 02 12.8	Sept. 01,60	7160	183	
203	2	Tonga Is.	15.1S 176.1W	14 16 52.4	〃 24,60	7290	92	
17	2	Samoa Is.	15 S 174.5W	20 14 27	Apr. 22,58	7400		6.5
14	3	Tonga Is.	17 S 173 W	21 09 09	Aug. 06,58	7670		6.5
45	2	Samoa Is.	16 S 172 W	17 44 48	Nov. 16,58	7660		6.3

N: Characteristic number of Rayleigh wave dispersion.

the India Ocean. Corresponding to this, the region, *i.e.*, the curve "5" was selected as a "sub-continental" one.

Then, our purpose is to discover these four parts in each travelling path. The actual procedure taken is as follows. (The data of the shocks used in this work are given in Table 1.)

In the area A containing the Mariana Sea (see Fig. 5), the observed dispersion characters are all rather continental (almost all of them are from "4" to "6"). Therefore, the Mariana Sea, though the depth is mostly deeper than 4 km, cannot be supposed to be region "1", but must be "3" at least. Then, as a first approximation, nearly the whole of the area in the Mariana Sea was supposed to be region "3", and outside of it, the contour line of 1 km sea depth was taken as the boundary between the regions "5" and "7". Upon this division, the travelling-time of Rayleigh waves with a certain period along a certain path was calculated C. This was compared with the observed travel-time O. Then if C is much greater than O, for instance, corrections were successively made on the division. That is, the length of the higher velocity region in the path, "3" in the present case, must be decreased or the length of the lower velocity region "7" or "5" must be increased, ...etc.

For instance, for the case of a path from epicenter 29 to Tsukuba (see Fig. 4), the path was, as a first trial, divided into the regions "7", "5" and "3", by boundary lines marked by l and m in Fig. 4, referring to the sea depth countour lines of 1 km and 4 km respectively. In this case, X_1, X_3, X_5 and X_7 (the path lengths which belong to the regions "1", "3", "5" and "7" respectively along the path) become 3160 km, 280 km, 2410 km and 0 km respectively. As the group velocities of Rayleigh waves for the period of 30 seconds in the regions "7", "5", "3" and "1" have been observed to be 3.40 km/sec, 3.70 km/sec, 3.88 km/sec and 4.00 km/sec respectively, the travel-time C became $930+76+720+0=1628$ seconds, which is too much smaller than the observed one O, 1648 seconds. Then the value of X_3 was successively so decreased as to become the $O\sim C$ much smaller.

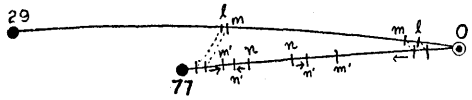

Fig. 4. Schematic figure which shows the method of discovering the boundaries of different regions. Along the path from 77 to the observed station O, the boundaries m and n which divide the regions (7, 5) and (5, 3) respectively were so moved as $m \rightarrow m'$ and $n \rightarrow n'$ in order to make the values of $O\sim C$ sufficiently small.

Next, in the case of the path from 77 to the observation station O, the boundaries which had been determined along the previous path were prolonged approximately parallel to the contour lines of sea depth.

In this case, however, the resultant dispersion characteristic number for this path is "3" which is remarkably more oceanic than the previous one ("6"). In order to explain this, the purely oceanic portion "1" was inserted along the path at a position in the deep sea region, deeper than 6 km. In this case also, the lengths belonging to each region were so chosen by the trial and error method as to make the value of $O-C$ sufficiently small.

These procedures were successively taken one by one for every path. Of course, the individual division itself along each path is not a unique one. But, if these boundaries being obtained on every path are reasonably connected to each other, we may say that the boundaries thus obtained are suitable as a first stage at least.

By connecting the corresponding division points on every travelling path, a map of the divided regions can be made, which is given in Fig. 5. For comparison, a chart is also given in the left, in which, in order to avoid complexity, the travelling paths are omitted. The path

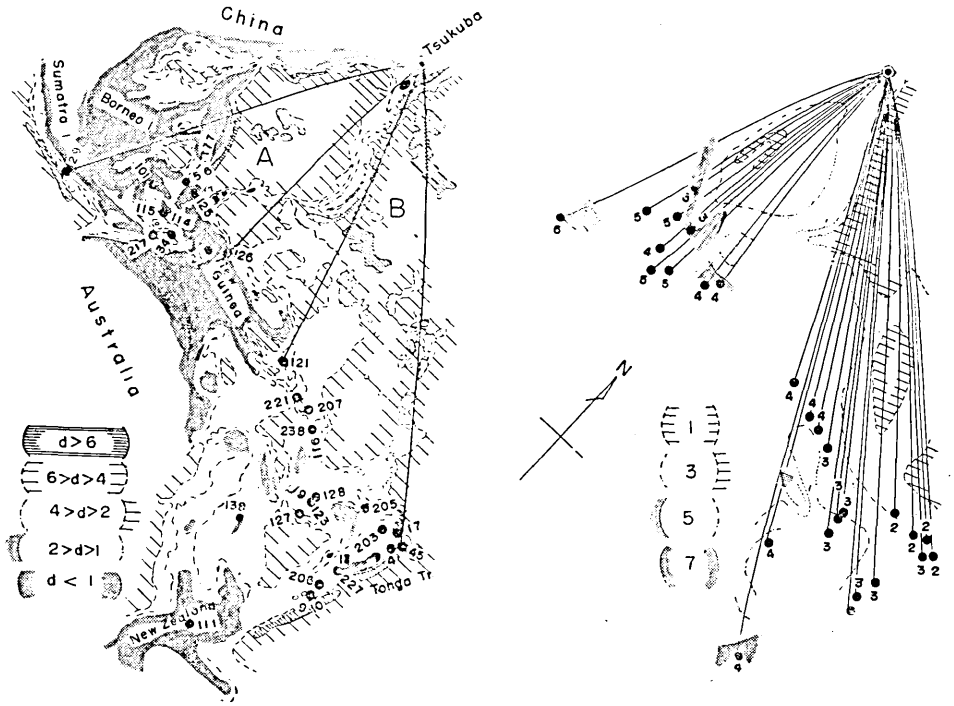

Fig. 5. A chart (left) and the map of the divided four regions in each of which Rayleigh waves have the same dispersion character. The number beside each epicenter in the chart means the shock number. d: sea depth in km.

lengths X_1, X_3, X_5 and X_7 belonging to each region, the observed travel-time C and the calculated one O along each path are given in Table 2.

As a check on this result, on the other hand, we can calculate the group velocities of Rayleigh waves in these four regions by the least square method as follows.

If the divisions were correct and thus, the dispersion characters were the same along every path in each region, we can write down the following k linear equations for every path for a given period T_0.

$$\left.\begin{array}{l} \dfrac{X_{11}}{V_1}+\dfrac{X_{31}}{V_3}+\dfrac{X_{51}}{V_5}+\dfrac{X_{71}}{V_7}=t_1(T_0) \\ \vdots \\ \dfrac{X_{1j}}{V_1}+\dfrac{X_{3j}}{V_3}+\dfrac{X_{5j}}{V_5}+\dfrac{X_{7j}}{V_7}=t_j(T_0) \\ \vdots \\ \dfrac{X_{1k}}{V_1}+\dfrac{X_{3k}}{V_3}+\dfrac{X_{5k}}{V_5}+\dfrac{X_{7k}}{V_7}=t_k(T_0) \end{array}\right\} \quad \cdots\cdots\cdots\cdots(1),$$

where X_{3j}, for instance, is the travelling path length belonging to the

Table 2.

"A" Group

No.	N	Δ (km)	X_1 (km)	X_3 (km)	X_5 (km)	X_7 (km)	t_{20} (sec)	t_{25} (sec)	t_{30} (sec)	t_{35} (sec)
29	(6)	5850	0	0	2890	2960	1880 (1848)	1720 (1715)	1640 (1648)	1590 (1609)
66	(3)	3550	1000	1140	1160	300	1040 (1037)	950 (958)	915 (932)	890 (918)
101	(5)	4500	400	1660	760	1680	1410 (1380)	1275 (1274)	1220 (1228)	1195 (1202)
56	(5)	4060	300	1560	1600	600	1230 (1214)	1120 (1121)	1080 (1085)	1060 (1065)
125	(3)	4080	850	2300	710	220	1180 (1184)	1070 (1091)	1050 (1059)	1030 (1046)
114	(4)	4700	850	1330	1710	810	1360 (1398)	1280 (1293)	1260 (1254)	1235 (1230)
115	(4)	4700	850	1330	1710	810	1360 (1398)	1280 (1293)	1260 (1254)	1235 (1230)
217	(5)	5010	0	1820	2020	1170	1520 (1509)	1370 (1401)	1350 (1359)	1340 (1329)
34	(5)	4780	0	1470	2590	720	1390 (1429)	1320 (1331)	1290 (1289)	1270 (1264)
21	(4)	4480	0	2750	1290	440	1270 (1314)	1210 (1224)	1180 (1189)	1155 (1167)
126	(4)	4390	0	2200	1890	330	1310 (1291)	1190 (1203)	1160 (1166)	1140 (1146)

(to be continued)

(continued)

"B" Group

No.	N	Δ (km)	X_1 (km)	X_3 (km)	X_5 (km)	X_7 (km)	t_{20} (sec)	t_{25} (sec)	t_{30} (sec)	t_{35} (sec)
121	(4)	5110	620	1590	2220	680	1550 (1520)	1390 (1407)	1350 (1365)	1320 (1340)
221	(4)	5570	1200	870	2820	680	1650 (1648)	1570 (1531)	1500 (1486)	1450 (1461)
138	(4)	5650	1200	930	4620	900	2310 (2278)	2120 (2118)	2050 (2054)	1990 (2011)
207	(3)	5750	2200	430	2820	300	1613 (1653)	1570 (1574)	1500 (1517)	1450 (1488)
116	(3)	5950	2800	900	1870	380	1720 (1714)	1600 (1590)	1550 (1548)	1520 (1517)
216	(3)	5950	2800	900	1870	380	1700 (1714)	1580 (1590)	1530 (1548)	1510 (1517)
238	(3)	5950	2800	800	1870	380	1780 (1714)	1620 (1590)	1550 (1548)	1520 (1517)
127	(3)	7400	2600	1700	2600	500	2170 (2150)	2010 (1989)	1940 (1935)	1890 (1907)
119	(3)	7180	2800	2200	1900	280	2070 (2069)	1910 (1908)	1850 (1864)	1820 (1837)
122	(3)	7180	2800	2200	1900	280	2100 (2069)	1900 (1908)	1840 (1864)	1810 (1837)
111	(4)	9270	1040	1500	5450	1280	2800 (2769)	2565 (1567)	2460 (2479)	2400 (2435)
9	(3)	8500	3200	3500	1500	300	2400 (2437)	2250 (2250)	2200 (2193)	2160 (2167)
10	(3)	8500	3200	3500	1500	300	2430 (2437)	2260 (2250)	2200 (2193)	2180 (2167)
206	(3)	8480	3400	3200	1500	280	2390 (2398)	2220 (2213)	2120 (2166)	2080 (2136)
13	(3)	2100	4700	1700	1490	300	2300 (2300)	2100 (2126)	2060 (2078)	2020 (2054)
227	(3)	8100	4700	1700	1400	300	2320 (2300)	2120 (2126)	2080 (2078)	2050 (2054)
205	(2)	7160	4400	1900	1600	260	2010 (2022)	1880 (1868)	1810 (1829)	1780 (1807)
203	(2)	7290	5350	1250	500	190	2020 (2036)	1890 (1886)	1830 (1853)	1810 (1829)
17	(2)	7400	3800	3150	250	200	2060 (2098)	1920 (1938)	1870 (1887)	1850 (1863)
14	(3)	7670	3810	3160	400	300	2130 (2177)	1990 (2009)	1960 (1965)	1930 (1942)
45	(2)	7660	3810	3250	400	200	2190 (2167)	2000 (2001)	1940 (1952)	1920 (1932)

No: Shock number. N: Dispersion characteristic number.
X_i: Path length along the region "i" (in km).
Δ: Total path length (in km).
t_{20}: Observed and calculated (in bracket) travel-times for the Rayleigh waves with periods of 20 seconds.

region "3", being measured on the division map along the path between the epicenter j to the observation station, V_3 the group velocity of Rayleigh waves in the region "3" and t_j (T_0) the travel-time of Rayleigh waves with the period T_0 along the total path. From these equations,

we can calculate the four unknowns V_1, V_3, V_5 and V_7 for a given period from eleven equations in A area, from twenty-one equations in B area or thirty-two equations for the $A+B$ area respectively.

From the data given in Table 2, the following observational equations can be written.

$$
\begin{array}{ll}
 & T_0: \quad 20 \quad 25 \quad 30 \quad 35 \\
\text{area } A & \left\{\begin{array}{l}
0\frac{1}{V_1}+0\frac{1}{V_3}+2890\frac{1}{V_5}+2960\frac{1}{V_7}=1880,\ 1720,\ 1640,\ 1590 \\
1000\frac{1}{V_1}+1140\frac{1}{V_3}+1160\frac{1}{V_5}+300\frac{1}{V_7}=1040,\ 950,\ 915,\ 890 \\
400\frac{1}{V_1}+1600\frac{1}{V_3}+760\frac{1}{V_5}+1680\frac{1}{V_7}=1410,\ 1275,\ 1220,\ 1195 \\
\vdots \quad \vdots \quad \vdots \quad \vdots \quad \vdots \quad \vdots \quad \vdots \quad \vdots \\
0\frac{1}{V_1}+2200\frac{1}{V_3}+1890\frac{1}{V_5}+330\frac{1}{V_7}=1310,\ 1190,\ 1160,\ 1140
\end{array}\right. \\
\text{area } B & \left\{\begin{array}{l}
620\frac{1}{V_1}+1590\frac{1}{V_3}+2220\frac{1}{V_5}+680\frac{1}{V_7}=1500,\ 1390,\ 1350,\ 1320 \\
1200\frac{1}{V_1}+870\frac{1}{V_3}+2820\frac{1}{V_5}+680\frac{1}{V_7}=1650,\ 1570,\ 1500,\ 1450 \\
\vdots \quad \vdots \quad \vdots \quad \vdots \quad \vdots \quad \vdots \quad \vdots \quad \vdots \\
3810\frac{1}{V_1}+3250\frac{1}{V_3}+400\frac{1}{V_5}+200\frac{1}{V_7}=2190,\ 2000,\ 1940,\ 1920
\end{array}\right.
\end{array}
$$

.....(2).

The calculations were made for the following three cases: (1) for A area only, (2) for B area only and (3) for $(A+B)$ area. The values of V_1, V_3, V_5 and V_7 calculated from the equations (2) are given in Table 3, and are plotted in the dispersion diagrams of a_2 (for A area), b_3 (for B area) and a_2+b_3 (for $A+B$ area) in Fig. 6 respectively. In these cases, the calculated dispersion dots lie well, in the range of observational errors at least, around the corresponding four dispersion curves. Of course, the writer could not reach this satisfactory result at once. He also obtained some unsuitable results, which are shown in the diagrams of a_1, b_1 and b_2 in Fig. 6. In these cases, the discrepancy between the calculated dots and the observed dispersion curves was very large owing to the great values of $O\sim C$ along every path and

Table 3.

V / T_0	V_1 (km/s)			V_3 (km/s)			V_5 (km/s)			V_7 (km/s)		
		Cal.	Obs.		Cal.	Obs.		Cal.	Obs.		Cal.	Obs.
20 sec	A	3.69		A	3.48		A	3.56		A	2.99	
	B	3.66	3.65	B	3.52	3.45	B	3.34	3.35	B	2.72	3.00
	A+B	3.62		A+B	3.56		A+B	3.32		A+B	2.93	
25 sec	A	3.96		A	3.85		A	3.68		A	3.19	
	B	3.93	3.94	B	3.81	3.78	B	3.48	3.59	B	3.58	3.25
	A+B	3.90		A+B	3.87		A+B	3.56		A+B	3.28	
30 sec	A	4.02		A	3.93		A	3.68		A	3.45	
	B	4.03	4.00	B	3.90	3.88	B	3.70	3.70	B	3.52	3.40
	A+B	3.90		A+B	3.87		A+B	3.56		A+B	3.28	
35 sec	A	4.19		A	3.96		A	3.74		A	3.57	
	B	4.09	4.04	B	3.92	3.93	B	3.87	3.78	B	3.49	3.50
	A+B	4.04		A+B	3.90		A+B	3.72		A+B	3.42	

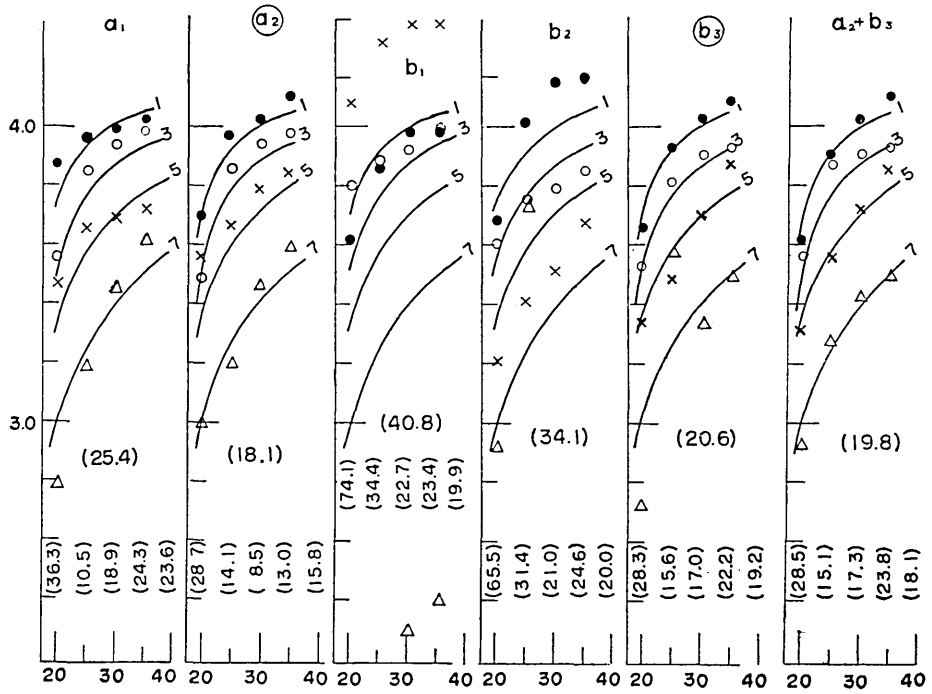

Fig. 6. Calculated dispersion data based on some unsuitable division (a_1, b_1 and b_2) and the final one (a_2, b_3 and a_2+b_3). The black and white circles, crosses and triangles mean the calculated group velocities in the regions "1", "3", "5" and "7" respectively and the smoothed curves mean the observed ones. The numbers in brackets above every period scale and in the centre are the standard deviations of $O\sim C$ in seconds for every period and for the whole periods respectively.

their large standard deviations for every period. (See Table 4 and diagrams in Fig. 6).

Table 4.

$O\sim C$ for "A" Group

	20 sec		25 sec		30 sec		35 sec	
	a_1	a_2	a_1	a_2	a_1	a_2	a_1	a_2
29	32	23	5	5	8	8	19	19
77	15	3	6	8	7	17	18	28
101	41	30	15	1	2	8	3	7
56	27	16	20	0	5	5	10	5
128	37	4	50	21	39	9	48	16
114	25	38	5	13	13	6	10	5
115	27	38	8	13	16	6	12	5
217	51	11	11	31	31	9	9	11
34	39	39	11	11	1	1	6	6
21	59	44	30	14	26	9	25	12
126	19	19	13	13	6	6	6	6
σ	36.8	28.8	10.5	14.1	18.9	8.5	24.4	15.8

$O\sim C$ for "B" Group

	20 sec			25 sec			30 sec			35 sec		
	b_1	b_2	b_3	b_1	b_2	b_3	b_1	b_2	b_3	b_1	b_2	b_3
121	136	86	30	23	23	17	19	19	15	8	8	20
221	68	54	2	84	74	39	51	43	14	34	14	25
138	147	96	32	60	34	2	43	25	4	13	7	7
207	197	197	40	42	42	17	17	17	17	20	38	38
116	27	27	6	10	10	10	2	2	2	3	3	3
216	7	7	14	10	10	10	18	18	18	7	7	7
238	87	87	66	30	30	30	2	2	2	3	3	3
127	45	45	20	21	21	21	5	5	5	17	17	17
119	36	36	1	2	2	2	14	14	14	17	17	17
122	61	61	1	8	8	8	24	24	24	27	27	27
111	89	31	31	22	22	2	9	9	19	23	35	35
9	2	31	31	0	0	0	7	7	7	7	7	7
10	38	38	37	10	10	10	7	7	7	13	13	13
206	29	29	7	7	7	7	34	34	34	56	56	56
13	18	18	8	50	26	26	28	18	18	46	34	34
227	32	32	0	30	30	6	8	8	2	6	6	4
205	24	24	20	0	0	12	27	27	19	6	6	34
203	5	5	16	70	4	4	36	23	25	34	19	19
17	3	38	38	18	18	18	17	17	17	13	13	13
14	10	47	47	33	19	19	15	5	5	15	15	12
45	64	23	23	1	1	1	12	12	12	12	12	12
σ	74.1	65.1	28.3	34.4	31.4	15.6	22.7	21.0	17.0	23.4	24.6	22.2

In Table 4, the $O\sim C$ for $T_0=20$ seconds are remarkably larger than those for other periods. This is owing to the large observational errors

in determining the group velocities in such a short period range where dV/dT is nearly infinitive.

From the final results a_2, b_3 and a_2+b_3 in Fig. 6, we may say that our division of the present area into such regions as is shown in the right map of Fig. 4 is quite a satisfactory one. It means, in other words, that if we divide the present area into such regions "1", "3", "5" and "7" as is shown in the right-hand map given in Fig. 4, all of the resultant dispersion character of Rayleigh waves observed at Tsukuba through the present area can be well explained.

3. Further investigations by using the seismograms at some other observation stations.

The figure of the divided regions, obtained by the method above given, is of course not exact. This method has an inevitable assumption about the kinds and numbers of fundamental regions. Even if the assumption we made were suitable, there remains the uncertainty about the shapes of divided regions due to the restricted dispersion data at the single station, Tsukuba. In other words, as the paths are all concentrated into a single station, the positions or the shapes of the divided region may have some radial uncertainty along the paths.

In order to remove this uncertainty and to correct the figures of regions or to discover some new boundaries which have been blind to the data at Tsukuba, dispersion data along other paths which, if possible, cross nearly perpendicularly the paths to Tsukuba Station are quite desirable. The most suitable stations for this purpose are Hongkong (China), Honolulu (Hawaii) and Suva (Fiji Is.) at which the same instruments as at Tsukuba, the Columbia-type seismographs, have been installed for the I.G.Y. and I.G.C. program.

The Lamont Geological Observatory, Columbia University, U.S.A. favoured the writer by sending him many copies of the seismograms recorded at these stations. From these copies, the writer was able to investigate into many such dispersive characteristics of Rayleigh waves resulting from shocks as are given in Table 5.

a) *General description about dispersion characteristics.*

Fig. 7 shows the dispersion data of Rayleigh waves along shorter paths (diagram (a)) and along longer ones (diagram (b)). From the dispersion characters shown in (a), the crustal conditions in the South

China Sea were newly ascertained. That is, the dispersion data of Rayleigh waves which pass over this area lie quite close along the continental curve "7". But, the dispersion data along the path, from the shock (250) to Hongkong which partly passes over the deep sea region at the middle of the Sea, lie close on the curve "5". This tells

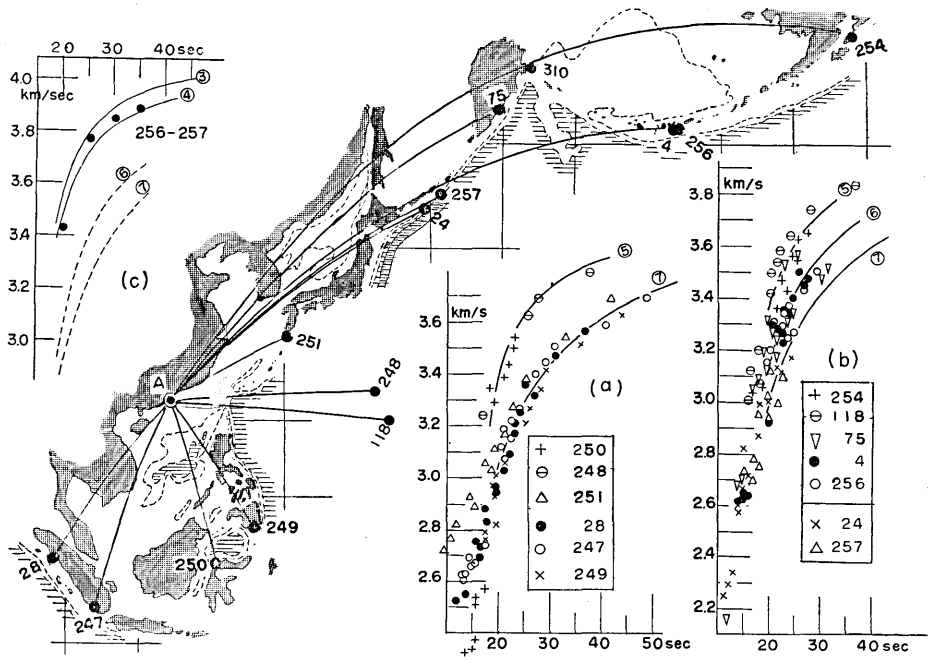

Fig. 7. Travelling paths of Rayleigh waves for Hongkong Station (A), and the dispersion data for every path (diagrams (a) and (b)). The black circles in (c) diagram represent the dispersion data being calculated by the subtraction of travel-times between the two epicenters (256) and (257).

us that there is an oceanic region somewhere in the middle of the South China Sea. The dispersion data of the shock (251) also lie close on the dispersion curve "7" for periods longer than 20 seconds, but they remarkably deviate from it in the short period range. The writer should like to postpone the explanation of this fact to some future time.

The dispersion data along the northern paths traversing the Japan Sea and the East China Sea were given in diagram (b). The dispersion data along the path resulting from the Kurile Islands shocks (24) and (257) lie close on the continental curve "7", though the dispersion data are missing for the periods longer than 25 seconds. On the other hand, in the dispersion data resulting from the Aleutian Islands shocks (4) and (256),

Table 5.

No.	N	District	Epicenter	Origin Time (G.M.T.)	Date	Δ (km)	h (km)	M
			Station: Hongkong					
4	6	Aleutian Is.	51.5N 176.5W	05h53m07s	July 01,58	6660	250	6
76	5	Bismark Sea	3 S 145.5E	18 01 05	Aug. 17,58	4440		
24	7	Kurile Is.	44 N 149 E	05 34 53	Nov. 14,58	4110		
75	6	Kamchatka	53 N 160 E	08 30 17	Oct. 10,58	5110		
211	5	Solomon Is. region	10.3S 161.2E	08 22 00.9	Oct. 22,60	6250	93	6.5
247	7	Sumatra I.	5 S 104 E	07 30 05	Dec. 02,59	6200	250	
249	5	Volcano Is.	24 N 141.5E	10 47 40	Feb. 23,58	2850		
249	7	Mindanao I.	5.5N 127 E	11 35 24	Oct. 10,58	2350		
250	5	Celebes I.	0.5S 120.5E	09 08 13	Apr. 22,58	2620		
252	5	New Britain	4.5S 153 E	19 12 36	Apr. 23,58	5150	100	
253	5	Tonga Is. region	24 S 176.5W	13 15 49	Sept. 14,59	9100		
256	6	Aleutian Is.	21.5N 176 W	09 08 35	Aug. 17,58	6650		
257	7	Kurile Is.	45 N 152 E	02 57 40	Apr. 23,58	4200		
28	7	Sumatra I.	2 N 98.5E	03 21 52	Oct. 12,59	2850		
320	4	Solomon Is.	5 S 154 E	14 56 57	May 1,59	5280		
99	6	Nicobar Is. region	7.9N 92.9E	20 40 06.5	Oct. 08,60	2780	84	
118	5	Mariana Is. region	22 N 144 E	18 38 10	Jan. 30,58	3060		
119	5	〃	21.5N 142.5E	17 56 05	〃	2920		
307	5	Near Hebrides Is.	13.5S 166 E	22 05 06	〃	6900		
310	7	Komandorskie Is.	55.7N 163.9E	05 35 21.0	Aug. 15 60	5360	25	
212	3	Indian Ocean	13.4S 65.8E	06 58 56.4	〃	6580		
213	3	〃	13.5S 67.0E	14 33 38.4	〃	6470		
206	4	Tonga Is. region	27.6S 176.9W	07 53 21.9	Sept. 01 60	9220	500	
205	4	Fiji Is.	16.1S 176.9W	20 02 12.8	〃	8350	184	
			Station: Honolulu					
77	3	Mindanao I.	7 N 126.5E	08 01 45	Sept. 11 58	8250		
19	2	Marshall Is.	12 N 165 E	03 29 58	July 12 58	4060		
9	2	Kermadec Is.	29 S 177 W	22 23 53	Sept. 14 59	8500		6.5
304	2	New Hebrides Is.	16.8S 167.6E	09 28 19.5	Sept. 01 60	5640		
308	2	〃	16.5S 167.6E	10 35 01.1	〃	5620		
138	2	Norfolk Is.	28 S 167.5E	11 12 31	May 20 60	6600		
297		Gulf of California	24 N 108 W	04 11 54	Mar. 06 60	5180		
125	2	Helmahera I.	1 N 129 E	02 22 06	〃	8260		
121	3	Solomon Is.	7.5S 156 E	21 37 05	Feb. 24 05	5920		
101	4	Celebes I.	1 S 123 E	09 34 00	Dec. 02 00	8940		
			Station: Suva					
319	5	Kermadec Is.	29 S 176.5W	10 15 17	Oct. 12 58	1310		
19	1	Marshall Is.	12 N 165 E	03 29 58	July 12 58	3660		
111	5	New Zealand	42 S 173 E	00 46 56	Feb. 21 60	2700		
77	5	Mindanao I.	7 N 126.5E	18 01 45	Sept. 11 58	6340		
29		Java I.	9.5S 112.5E	01 12 30	Oct. 20 58	7150		
28	6	Sumatra I.	2 N 28.5E	03 21 52	Oct. 12 59	8850		

the paths of which cover in addition the oceanic region between the Kurile and Aleutian Islands, lie also on the rather continental characteristic curve "6". As the path resulting from the shock (257) runs quite near the path of the shock (256), we can obtain the dispersion curve for the remaining part, from (256) to (257) by the subtraction of

the travel-times for every period. The result is shown in the diagram (c) given at the left upper part of Fig. 7. This result tells us that the dispersive characteristic number for the region along the path between the two epicenters (256) and (257) is approximately "4". The path from (256) and (257) includes sea region deeper than 4 km which occupies approximately 3/5 of the total path. On the other hand, the dispersion curve "4" can be obtained when Rayleigh waves passed across the regions "3", "2", "1" and "5", "6", "7" with the path length ratio of 3 : 2 respectively. Therefore, if the region deeper than 4 km along the path is region "3", "2" or "1", the remaining part must be region "5", "6", or "7" in this order respectively. Regrettably, the writer does not have sufficient knowledge about the crustal structure of these regions to select a suitable pair among these three cases. But, the first case, *i.e.*, the characteristic number for the region deeper than

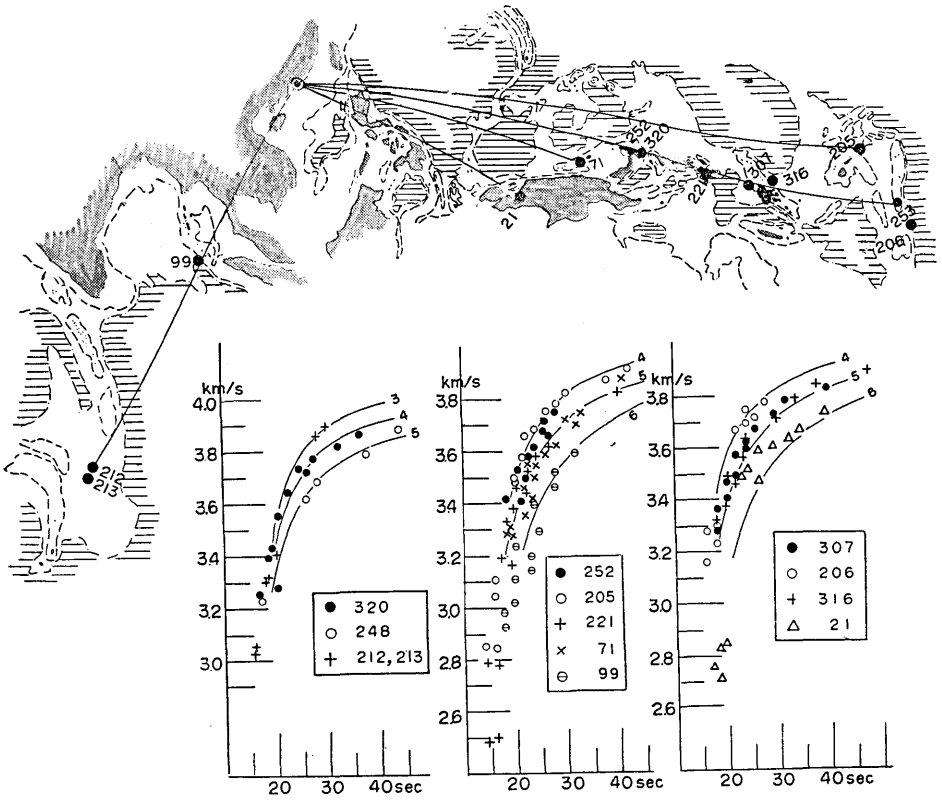

Fig. 8. The dispersion data at Hongkong and the corresponding paths over the complicated area.

4 km along the present path is in an average "3" and accordingly, that for the remainder region is in an average "5" seems to be the most natural.

The dispersion data and the corresponding paths which cover the complicated area are given in Fig. 8 (Hongkong Station), Fig. 9 (Honolulu Station) and Fig. 10 (Suva Station).

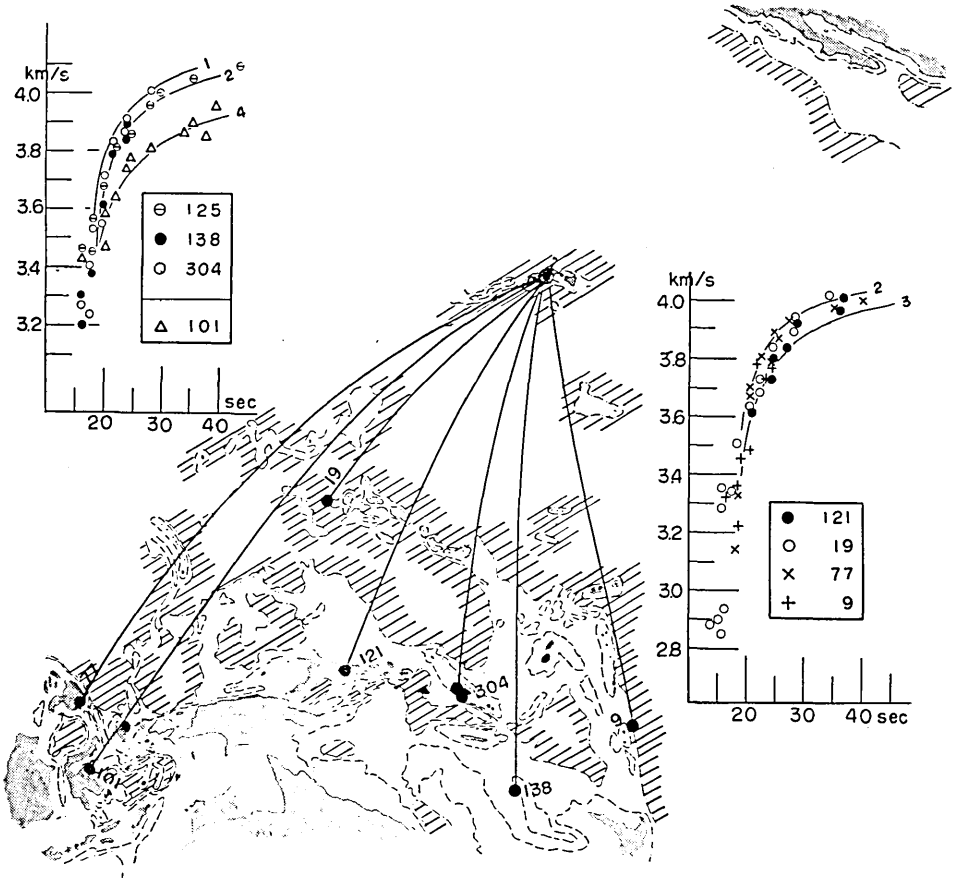

Fig. 9. The dispersion data at Honolulu and the corresponding paths over the complicated area.

b) *Use of the new data.*

The dispersion data given in Figs. 8, 9 and 10 are quite valuable for checking the division map which was made by the dispersion data at Tsukuba. Besides, they can be used to find some new boundaries of the regions for which the Tsukuba data were missing. The paths here used are shown in the left chart of Fig. 11, and the revised map of

the divided regions, based upon the supplementary data, is given on the right hand. The method adopted was quite the same as the previous one. That is, to divide each travelling path into such sections in order to

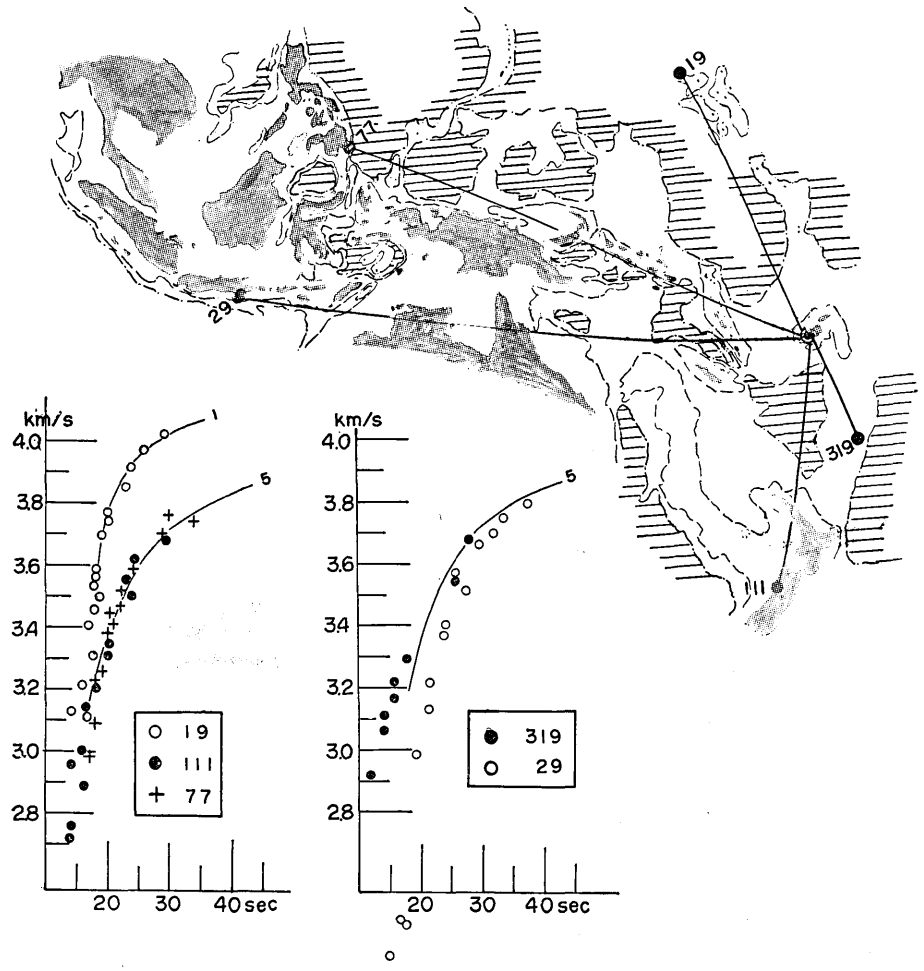

Fig. 10. The dispersion data at Suva and the corresponding paths over the complicated area.

make the differences between the two travelling times $O\sim C$ along each path sufficiently small. In these trials, the previous result, together with the topographical conditions was of course considered. For instance, along the path from 248 (Mariana Is. shock) to Hongkong, the travel distances which cover the regions "1", "3", "5" and "7" becomes 0 km, 830 km, 780 km and 1240 km respectively if we measure them on

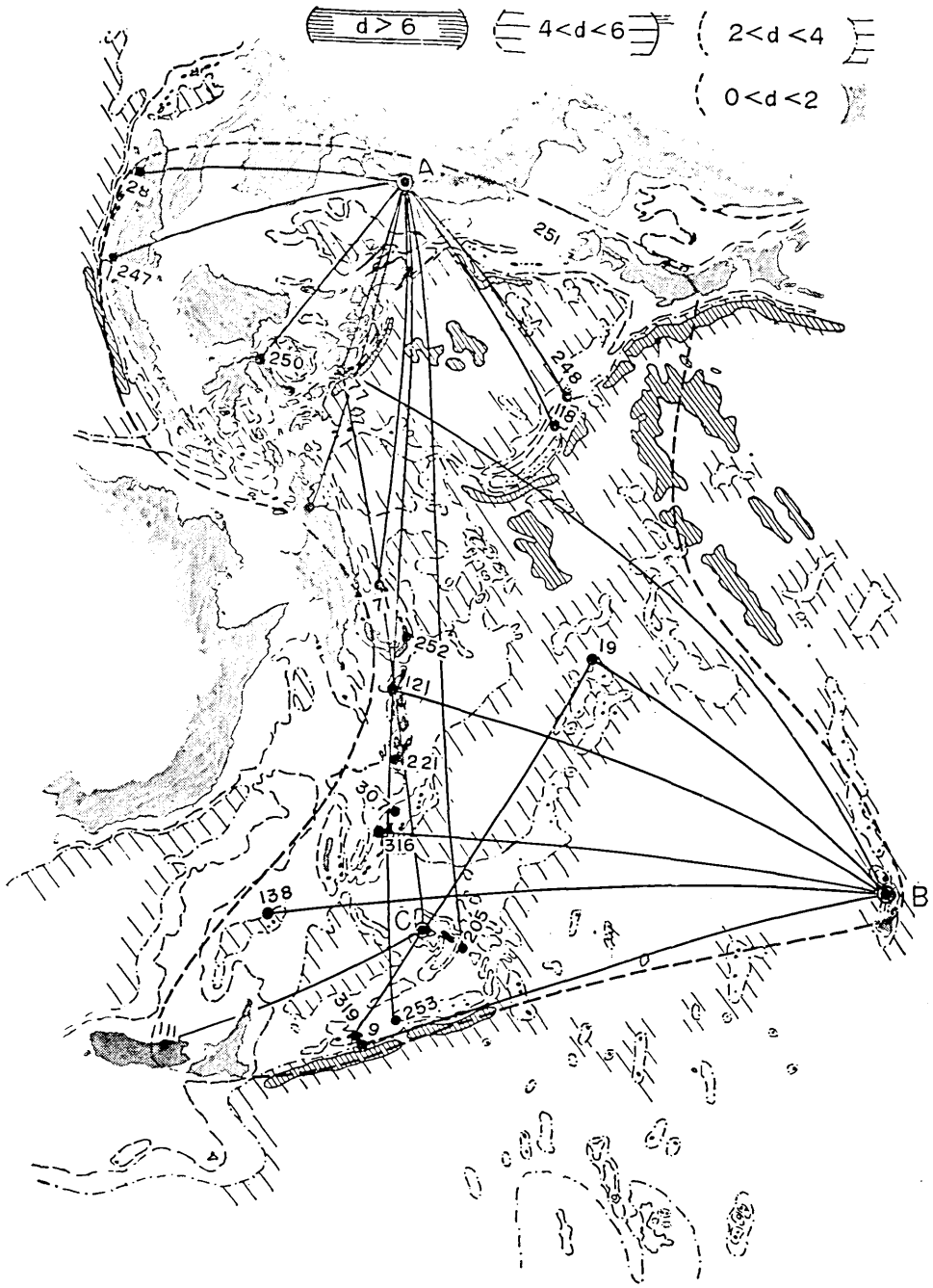

Fig. 11. A division map revised by the new data at Hongkong (A), Honolulu (B) and are the areas deeper than 6 km and broken and chain lines mean the contour line of the

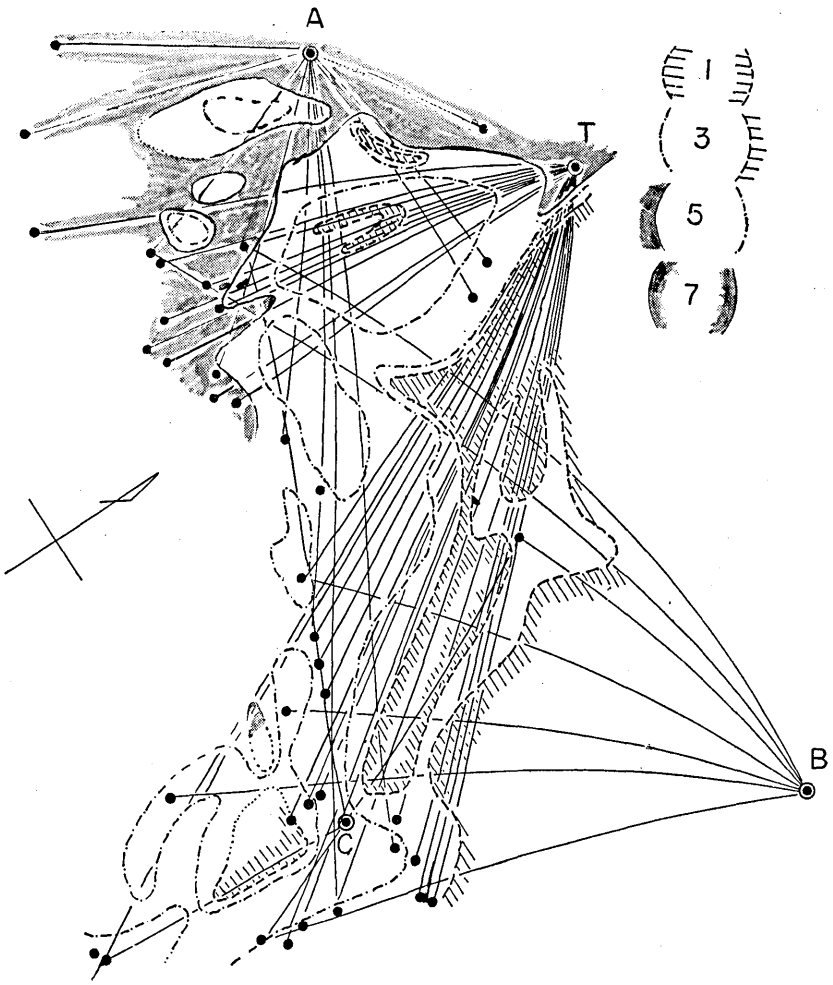

Suva (C), and the ordinary chart of the same area (left). In the left chart, hatched regions depth of 2 km and 4 km respectively.

the division may previously drawn up. If so, the travel-time of Rayleigh waves with the period of 30 seconds along this path was calculated as 789 seconds, which was too large as compared with the observed one, 766 seconds. In order to decrease the difference between these two values, the region "1" was added at the Ryukyu Trench position. After that, the lengths of four regions were successively changed, and the value of C could be reduced to 768 seconds at last by the values of X_1, X_3, X_5 and X_7 as 450 km, 1060 km, 500 km and 840 km respectively. The same procedures were carried out along all the paths. The numerical results are given in Table 6, in which X_i represents the travelling path length of Rayleigh waves across the region "i" and t_{20} for instance, represents the observed and calculated (in brackets) travel-times of Rayleigh waves with the period of 20 seconds respectively. The values

Table 6.

No.	N	Δ (km)	X_1 (km)	X_3 (km)	X_5 (km)	X_7 (km)	t_{20}	t_{25}	t_{30}	t_{35}
Station: Hongkong										
205	4	8350	770	4040	2980	560	2420 (2458)	2260 (2266)	2200 (2202)	2165 (2166)
307	5	6900	0	3630	2390	880	2040 (2058)	1890 (1898)	1840 (1841)	1810 (1808)
118	5	3060	250	1510	510	790	890 (921)	840 (848)	815 (821)	805 (806)
248	5	2850	450	1060	500	840	843 (859)	792 (793)	766 (768)	752 (753)
253	5	9100	150	2480	4740	730	2640 (2790)	2480 (2508)	2430 (2430)	2400 (2387)
221	5	6250	150	2670	2700	730	1850 (1865)	1730 (1723)	1680 (1672)	1650 (1637)
71	5	4400	0	1980	1500	920	1298 (1281)	1222 (1230)	1183 (1185)	1159 (1167)
21	6	3680	230	0	1200	2150	1200 (1136)	1060 (1054)	1020 (1015)	997 (989)
Station: Honolulu										
121	3	5920	3960	980	980	0	1670 (1660)	1540 (1540)	1510 (1506)	1490 (1489)
19	2	4060	3350	710	0	0	1160 (1139)	1060 (1039)	1020 (1021)	1010 (1012)
77	3	8250	5400	1890	890	70	2300 (2371)	2130 (2141)	2085 (2078)	2070 (2071)
Station: Suva										
319	5	1310	0	650	660	0	385 (385)	360 (361)	350 (349)	305 (313)
77	5	6340	80	1850	4050	360	1870 (1888)	1730 (1753)	1700 (1692)	1660 (1666)

of $O\sim C$ are given in Table 7. The regions thus obtained are shown in the right map of Fig. 11.

Table 7.

	No. \ T	20 sec	25 sec	30 sec	35 sec
Hongkong	248	16	1	2	1
	253	51	28	0	13
	252	16	6	5	—
	221	15	7	8	13
	250	35	22	2	—
	71	17	8	2	9
	205	38	6	2	1
	307	18	9	1	0
	118	29	13	7	2
	21	64	7	7	8
Suva	319	0	3	5	8
	111	8	3	4	—
	77	17	20	3	6
	19	33	3	5	—
Honolulu	121	10	7	4	2
	138	15	9	—	—
	19	23	21	2	3
	9	8	1	—	—
	77	17	11	7	1
	σ	27.0	12.1	4.4	6.4

As before, the group velocities of Rayleigh waves in every region were calculated by means of the least square. In this case, not only the numerical data newly obtained but also the data at Tsukuba Station (Table 2) were used. Therefore, the least square method was carried out by observational equations as many as forty-five in all.

The group velocities in every region thus obtained are given in Table 8, and they are plotted on dispersion diagrams in Fig. 12. Judging from the result which shows that the calculated dots lie close, at least in the range of observational errors, on the observational dispersion curves "1", "3", "5" and "7", we can say that our division map is quite satisfactory for explaining all of the Rayleigh waves dispersion characteristics along forty-five paths.

Comparing the revised division map (right map of Fig. 11) with the previous one (Fig. 5), the following points can be noticed.

I) The area west of the Philippines, Mindanao Island and north of Celebes Island, was newly divided into some regions. The effect of the existence of a rather deep sea regions at the South China Sea and the Celebes Sea appears on the dispersion character along the path from the epicenter (250) to Hongkong.

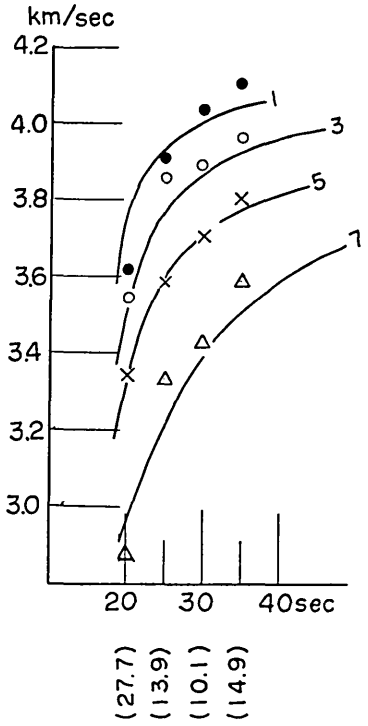

Fig. 12. Calculated dispersion data for the divided four regions and the assumed dispersion curves. The marks of the calculated dots are the same in Fig. 6. Numbers in bracket under the period scale mean the standard deviations of $O-C$ for the corresponding periods.

II) The area around the Ryukyu Islands which also had been left blank was divided. The existence of the Ryukyu Trench also had remarkable effect upon the dispersion character along the paths from (248) and (118) to Hongkong.

III) The sub-oceanic region "3" which was postulated in the Caroline Sea was enlarged eastward in order to explain the dispersion characteristics along the paths from (121), (221), (252), (71), (253) and (205) to Hongkong.

IV) In the Mariana Sea, the shape of region "3" was slightly extended westward. The location and the shape of region "1" could not be sufficiently investigated from the new data.

V) The isolated purely oceanic region "1" which was situated in Micronesia was greatly extended from the Fiji Islands to the Marshall Islands in order to explain the dispersion feature along the path from the epicenter (19) to Suva (C).

VI) The dispersion character in the broad sea area northeast of a

Table 8.

V (km/s) / T (sec)	V_1		V_3		V_5		V_7	
	Cal.	Obs.	Cal.	Obs.	Cal.	Obs.	Cal.	Obs.
20	3.61	3.65	3.54	3.45	3.34	3.35	2.87	3.00
25	3.90	3.94	3.86	3.78	3.58	3.58	3.33	3.25
30	4.04	4.00	3.98	3.88	3.70	3.70	3.42	3.40
35	4.11	4.04	3.89	3.93	3.90	3.78	3.59	3.50

line from the Tongas up to Hawaii, belongs to "1", which is the same as those in the ordinary Pacific Ocean.

4. Crustal models which satisfy the four dispersion curves

The most important problem is that what kind of crustal model can explain each of four dispersion curves in the divided region "1", "3", "5" and "7" respectively.

R. Yamaguchi *et. al.*[4] calculated the theoretical dispersion curves of Rayleigh waves along various crustal models being covered with water. From their results, four models T_1, T_3, T_5 and T_7 given in Fig. 13 were selected as suitable ones which respectively fit best for our

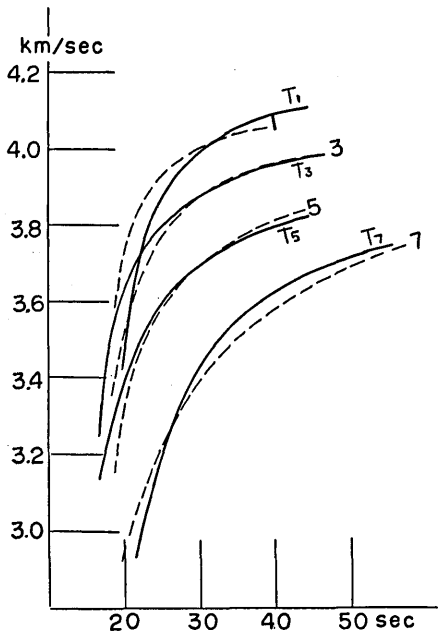

T_1

α	ρ	h
1.52	1.00	6.0
6.90	2.67	6.0
8.10	3.00	∞

T_5

α	ρ	h
1.50	1.00	3.0
5.50	2.80	12.0
7.80	3.00	∞

T_3

α	ρ	h
1.50	1.00	4.5
6.00	2.80	6.75
7.95	3.00	∞

T_7

α	ρ	h
1.50	1.00	0.9
5.00	2.80	18.0
7.95	3.00	∞

Fig. 13. Observed dispersion curves (broken curves) "1", "3", "5" and "7" in the divided regions and the theoretical curves (solid curves) for the models of T_1, T_3, T_5 and T_7 which are given in the right hand.

four observed dispersion curves "1", "3", "5" and "7". The mean value of water depth measured along all of the paths in the region "1" was around 6.8 km. But, as the calculations of the dispersions for

4) R. YAMAGUCHI and T. KIZAWA, "Surface Waves and Layered Structure (Part II)," *Bull. Earthq. Res. Inst.*, **39** (1961), 669.

the crustal models with such deep water layer had not been done, the writer had to compare the observed curve "1" to a theoretical dispersion curve for the model with the water layer of 6 km. If we increase the thickness of the water layer and decrease that of the crust, however, the calculated curve T_1 must be shifted leftward, and the discrepancy between two curves T_1 and "1" will become much smaller. The depth of the water layer in other three models were taken as mean values of those along all of the paths which cover each divided regions respectively.

From these results, we can say at least that the shift of the dispersion curves in these four regions can be explained by both decreasing of the compressional wave velocity in the crust and by increasing the thickness of the crust. As was suggested in the previous paper[5], the decreasing of compressional wave velocity in the crust may be caused by the existence of volcanic layers in the crust in the present area.

5. Conclusions

Intricated structured area in the western side of the "Andesite line", embrasing the Mariana Sea, Micronesia, or Melanesia, was divided into four regions in each of which the dispersion character of Rayleigh waves show the characteristic numbers "1", "3", "5" and "7" respectively.

The first division map was drawn up by using the dispersion data of Rayleigh waves observed at Tsukuba Station along thirty-two paths across the area. Next, this map was somewhat corrected by the addition of thirteen new dispersion data for three other stations, Hongkong, Honolulu and Suva.

These results were checked by calculating the group velocities in every region by the least square method, and it was found that our result was quite satisfactory as all of the resultant dispersion data along forty-five paths across the area were well explained.

Four crustal models which respectively fit the four dispersion curves "1", "3", "5" and "7" were selected, and it was found that the shift of the dispersion character from "1" to "7" could be explained by decreasing the compressional wave velocity in the crust from 6.9 km/sec to 5.0 km/sec and by increasing the thickness of the crust from 5 km to 20 km.

I) As was found in the previous papers, the dispersion character

5) *loc. cit.* 3).

across the sea deeper than 4 km in the Central Pacific Ocean was "1". This circumstance, however, changes in the western side of the "Andesite line". In this area, the dispersion character in the sea deeper than 4 km becomes "3" instead of "1". Roughly speaking, the region "1" in this area, seems to be limited to the regions deeper than 6 km.

II) In the area west of the Philippines, Mindanao Island and north of Celebes Island, the sub-oceanic region "3" could be found only at two locations, the first is at the central part of the South China Sea and the other at the Celebes Sea.

III) Four kinds of dispersion curves in the divided regions were compared with the theoretical ones, and it was found that the shift of the dispersion character from "1" to "7" in the divided regions can be explained by decreasing the compressional waves velocity in the crust from 6.9 km/sec to 5.0 km/sec and by increasing the thickness of the crust from 5 km to 20 km. The decreasing of the compressional wave velocity in the crust in the present area may be, as was suggested in the previous paper, caused by the existence of volcanic layers.

6. Acknowledgement

In the course of the writer's investigations into the dispersion character of Rayleigh waves including the previous three papers, he was greatly indebted to Prof. T. Hagiwara who allowed him to use the abundant records of seismograms recorded at Tsukuba Station under his supervision. The indefatigueable effort of the observational staff of the station including Mr. M. Watanabe must be highly acknowledged.

The writer wishes to express his hearty thanks to Prof. C. Tsuboi who gave him valuable advice and discussed with him the methods of finding regional group velocities from abundant dispersion data.

The Lamont Geological Observatory, Columbia University, U.S.A. helped the writer by sending many copies of seismograms obtained at Hongkong, Honolulu and Suva. The writer's cordial thanks are due to all the people concerned in these institutes and stations.

In selecting some suitable crustal models which fit well for our observed dispersion curves, the writer is greatly indebted to Mr. R. Yamaguchi.

Finally, it must be added that all of the calculations by the least square method were made at the Yulin Computing and Processing Centre, Tokyo.

23. 西南太平洋海域を，夫々の内部でレーリー波が同一の群速度を示す様ないくつかの地区に分けること

東大地震研究所　三　東　哲　夫

前論文で，海洋を伝わつて日本にやつてくるレーリー波の分散曲線を7種に分類したが，これらの分散曲線は，実は夫々独立なものではなくて，例えばレーリー波が，夫々の内部では“1”，“4”，“7”という分散特性を示す様な領域を夫々 3:3:4 の割合で含む径路を通つてきた場合には，全体としての分散特性は“5”になる，といつた具合に，お互いに関連性をもつていることも前論文で示されている（第3図）．この事実を逆に利用することによつて，西南太平洋，特にいわゆる安山岩線の西側の海域を，レーリー波が全く陸的な分散を示す海域“7”，かなり陸的な分散を示す海域“5”，かなり海的な分散を示す海域“3”，完全に海的な分散を示す海域“1”の4つの領域に分割することを試みた．先ず最初は，東大震研の筑波支所の記録から得た合計32本の径路に沿つての分散資料を用い（第4図），次に，これらの径路と交叉する径路をとるものとして，香港，ハワイ，フィジー島の3ヶ所における記録から調べた計13ヶのレーリー波の分散資料を加えて，それによつて前の結果に若干の補正を加えた（第11図）．

逆に，この様にして分けられた4つの領域内でのレーリー波の群速度を各周期毎に最小二乗法で求めて見ると，始めに仮定した各領域内のでそれらと，少くとも観測の誤差範囲内でかなりよく合うことが示された（第12図）．

こうして得られた分散図から判断すると，安山岩線の西側は東側に比べてたしかに全体として陸的な構造になつている様に思われる．即ち，東側では，海深4キロ以上の場所ではレーリー波は分散特性“1”，つまり純海洋的な分散特性を示すのに，西側では同じ深さの場所は，やや海的な特性“3”になつている．そして西側で“1”を示すのは僅かに深さ6キロ以上の深海部分に限られている．

また，東支那海，ボルネオ海等を通るレーリー波は，完全に陸的な分散特性“7”を示す．この附近でやや海洋的なのは，僅かに南支那海の中央部と，セレベス海の一部（共に“3”）である．

最後に，これら4種の分散特性“1”，“3”，“5”及び“7”を示す各領域が，どんな地殻構造のモデルで説明できるかを調べて見ると，大凡ではあるが，上部でのP波の速度が約8 km/s である様な中間層の上に，その内部でのP波の速度，及び厚さが夫々“1”では 6·9 km/s で 5 km，“3”では 6 km/s で 7 km，“5”では 5.5 km/s で 12 km，“7”では 5.0 km/s で 20 km 程度の値をもつ地殻をのせたものになる（第13図）．前の論文でも指摘したように，地殻内におけるP波の速度の減少は，おそらく海底火山の溶岩層の存在に原因しているのではないかと思う．